First-principles investigation of structural and magnetic disorder in CuNiMnAl and CuNiMnSn Heusler alloys

S. Aron-Dine, G. S. Pomrehn, A. Pribram-Jones, K. J. Laws, and L. Bassman

Phys. Rev. B **95**, 024108 — Published 10 January 2017

DOI: 10.1103/PhysRevB.95.024108

First principles investigation of structural and magnetic disorder in CuNiMnAl and CuNiMnSn Heusler alloys

S. Aron-Dine,[1] G.S. Pomrehn,[2] A. Pribram-Jones,[3,4] K.J. Laws,[5] and L. Bassman[1]

[1] *Harvey Mudd College, Claremont, CA 91711, USA*
[2] *The Boeing Company, Seattle, WA 98108, USA*
[3] *Lawrence Livermore National Laboratory, Livermore, CA 94550, USA*
[4] *Department of Chemistry, University of California, Berkeley, CA 94720 USA*
[5] *School of Materials Science and Engineering, UNSW Australia, Sydney, NSW 2052, Australia*

(Dated: December 16, 2016)

Two quaternary Heusler alloys, equiatomic CuNiMnAl and CuNiMnSn, are studied using density functional theory to understand their tendency for atomic disorder on the lattice and the magnetic effects of disorder. Disordered structures with anti-site defects of atoms of the same and different sub-lattices are considered, with the level of atomic disorder ranging from 3%–25%. Formation energies and magnetic moments are calculated relative to the ordered ground state and combined with a simple thermodynamical model to estimate temperature effects. We predict the relative levels of disordering in the two equiatomic alloys with good correlation to experimental XRD results. The effect of swaps involving Mn is also discussed.

I. INTRODUCTION

Heusler alloys have strong potential for use in spintronics applications. They are of particular interest for developing giant magnetoresistance and giant tunneling magnetoresistance spin valves since they often behave as half-metallic ferromagnets[1–5]. Their high spin polarization can be exploited to act as a conductor for correctly aligned spins and an insulator for incorrectly aligned spins[6]. Candidate materials for these applications must be ferromagnetic, have a high Curie Temperature and have robust spin polarization. Ideally these materials would be 100% spin polarized at the Fermi level, but lower levels of spin polarization are still adequate for developing spintronic devices[7]. Previous experimental and computational investigation of ternary full-Heusler alloys of the form X_2YZ involving the elements Cu, Ni, Mn, Al, and Sn show promising properties[8–10].

In their analysis of magnetic behavior of Mn-based Heusler alloys, Kubler et al.[1] found that when the X and Z elements of a Heusler structure are nonmagnetic, the magnetization is almost completely confined to the Mn atoms, and the Z element often couples the Mn-to-Mn interactions. If the X element is Co or Ni, there is an additional magnetization on these lattice sites. The five paramagnetic d electrons in ground-state Mn undergo spin-flip processes due to significant electronic interactions during bonding with X atoms. This energetic separation of electrons with different spins results in a magnetic moment highly localized on Mn atoms. This interaction is also what is believed to result in high spin polarization at the Fermi level.

Although many Heusler alloys have been predicted to be 100% spin polarized ferromagnets with large magnetic moments from first principles calculations, very few have exhibited such behavior in experiment[14–17]. The alloys almost always have substantially lower magnetization and polarization than predicted — beyond what might be expected from computational uncertainties. A proposed mechanism to explain this behavior is atomic disordering[2]. Since the specific ordering of atomic species on the lattice is integral to electronic properties, the magnetic properties of a Heusler alloy have a high sensitivity to anti-site defects[1].

Recent development and characterization of a new family of high entropy brasses and bronzes produced two new quaternary Heusler alloys, CuNiMnAl and CuNiMnSn ($Cu_{2-x}Ni_xMnZ$ where $x = 1$)[11]. It is not surprising that these compositions exhibit Heusler structure since Cu_2MnAl, Cu_2MnSn, Ni_2MnAl, and Ni_2MnSn all exhibit classic full X_2YZ Heusler structure and ferromagnetic behavior[12]. The high entropy brass and bronze alloys both exhibit $L2_1$ structure with a 16-atom unit cell where Cu occupies the (0,0,0) sites, Ni occupies the ($^1/_2$, $^1/_2$, $^1/_2$) sites, Mn occupies the ($^1/_4$, $^1/_4$, $^1/_4$) sites, and Al or Sn occupies the ($^3/_4$, $^3/_4$, $^3/_4$) sites.

Experimental investigation of these alloys included X-ray crystallography (XRD) to determine the structures and lattice parameters of the heat-treated alloys. Although the two alloys have the same overall lattice structure, many more peaks are present in the trace for CuNiMnSn than the trace for CuNiMnAl (Fig. 1). This difference can be partially accounted for by the difference in atomic species in each alloy, but the striking difference between the two, persistent in higher resolution scans, indicates that the CuNiMnAl alloy exhibits more atomic disorder on the lattice than the CuNiMnSn alloy. This atomic disordering reduces the longer range ordering of the material and hence the number of reflections present in the XRD trace[13]. The properties of a Heusler alloy are highly dependent on its atomic structure, meaning that small changes in the arrangement of atoms on the lattice can have a substantial effect on its electronic properties[1]. With experimental evidence that CuNiMnAl has a higher level of disordering than CuNiMnSn, these two alloys are good candidates for computational study to understand the nature of anti-site defects in Heusler alloys and how

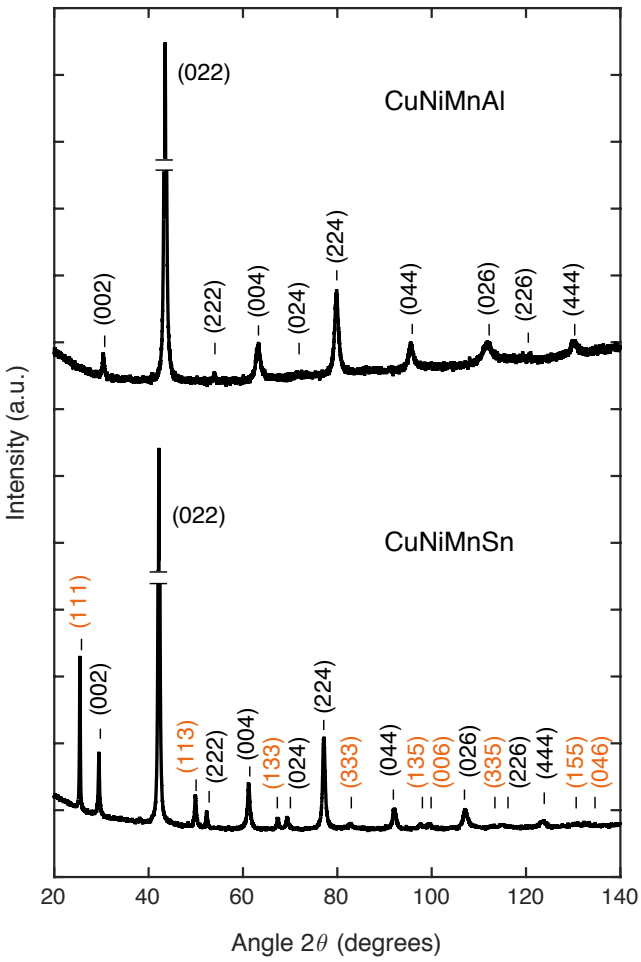

FIG. 1. XRD traces for CuNiMnAl and CuNiMnSn heat-treated alloys. Powder XRD was performed using the PANalytical Xpert Multipurpose X-ray Diffraction System using a Cu Kα radiation source. Samples were prepared using a ring mill. Both scans were performed using identical machine settings. Additionally, longer scans were performed on the CuNiMnAl sample which did not reveal additional reflections. Adapted from Ref.[11].

electronic properties are affected.

Miura et al. predicted that substitutions between atoms on different sub-lattices of $Co_2Cr_{1-x}Fe_x$ reduce the magnetic moment and spin polarization much more than substitutions on the same sub-lattice[18]. They also found that structures with swaps between atoms on different sub-lattices have a much higher ground-state energy (a difference as large as 3 eV) and concluded that they were therefore unlikely to be energetically accesible at experimental temperatures[19]. Similarly Gerci and Hono studied the effect of structural disorder on theoretical spin polarizations and magnetization in ternary $Co_{2.25-x}Fe_{0.75+x}Si$ alloys[20]. They found that these disordered structures have consistent and significantly higher energies of formation, between 0.4-1.75 eV/atom. However, they used small (16-atom) unit cells in their simulations and were limited to studying two levels of B2 type disorder, 25% and 50%. In addition Hasnip et al. found that in Co-based Heusler alloys the half-metallicity depends strongly on the type of lattice swapping present[21]. However they only considered high levels of disorder ($> 25\%$) and concluded that since the formation energies of XY and YZ disordered structures were quite large they could be removed by annealing the material. No study to date has looked at the interaction between temperature and disordering behavior.

In this work we present a study of increasing levels of atomic disorder—from 3% to 25%— in the CuNiMnAl and CuNiMnSn equiatomic alloys for all possible types of atomic swaps. We combine these calculations with a simple thermodynamic model to predict the extent of atomic disorder at observable temperatures and expected reduction of magnetization as a function of temperature.

II. COMPUTATIONAL METHODOLOGY

A. Simulating disorder

For a quaternary Heusler alloy there are six types of atomic disorder. These can be classified as swaps of elements residing on the same sub-lattice or on different sub-lattices. In this work we explore five levels of atomic swapping (3.125%, 6.25%, 9.375%, 12.5%, 25%) for all six types of swaps for each quaternary alloy. This focus on single types of swaps may be artificial, but it is an effective tool for isolating the effects of each type of atomic swap (same vs different sublattice). The disordered structures are approximated using 128-atom special quasirandom structures (SQSs) designed to match—in a periodic supercell— the nearest and second-nearest neighbor interactions expected if the disordered sites were randomly distributed throughout the alloy[22]. The structures were created using a Monte-Carlo method implemented in the Alloy Theoretic Automated Toolkit[23,24].

Figure 2 shows an example of a unit cell for a disordered structure compared with an ordered Heusler unit cell. Since an SQS is not an exact representation of ran-

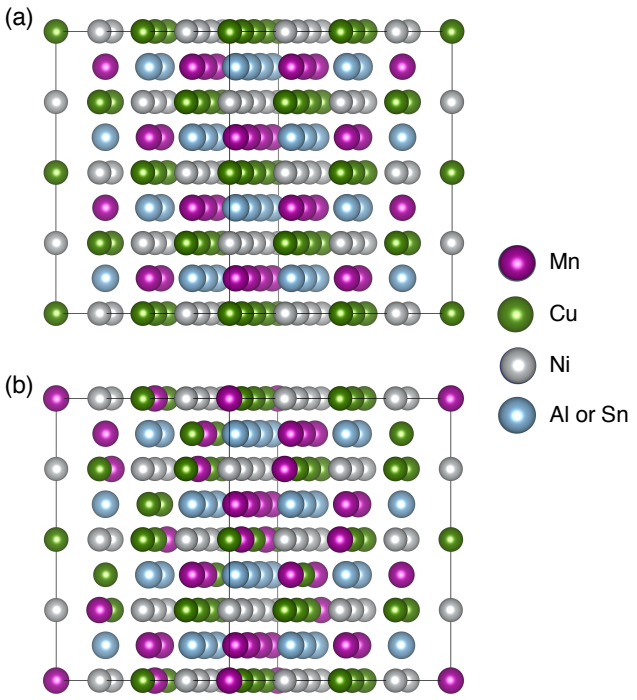

FIG. 2. A 128-atom quaternary Heusler cell with (a) ordered structure and (b) 25% of the Cu and Mn atoms swapped. Visualization created using the VESTA software package[25].

domly distributed disorder in an alloy, we generated three unique SQSs, three realizations for each level of disorder, to estimate the level of uncertainty in our method. This is a new method to investigate the robustness of computational results.

B. Density Functional Calculations

The total energies of the perfectly ordered quaternary structures were calculated with the Vienna Ab-Initio Simulation Package (VASP)[26] using PBE pseudopotentials[27], using a range of lattice parameters. The calculations were converged with a Monkhorst Pack $4 \times 4 \times 4$ k-point mesh and a plane wave energy cutoff of 450 eV. The energies—as a function of lattice parameter—were then fit to the Birch-Murnaghan equation of state for isotropic solids to determine the lowest energy ground-state lattice parameters[28]. Table I shows good agreement between the computationally determined lattice parameters and the lattice parameters determined by XRD. Discrepancies between the two of a few percent are to be expected when using GGA pseudopotentials[29]. The ground-state lattice parameter was then consistently used for each of the disordered structures. This is a common practice since the volume of the unit cell changes a negligible amount due to atomic disordering[20,21]. The formation energy and magnetic moment for each of the disordered structures was found using VASP, allowing for a full relaxation of atomic positions. For local density of states calculations, an $8 \times 8 \times 8$ k-point grid was used.

TABLE I. Experimentally and computationally determined lattice parameters

Lattice Parameter (Å)	CuNiMnAl	CuNiMnSn
XRD	5.89	6.08
Computation	5.86	6.02

C. Thermodynamic Model

A simple model for the configurational entropy was combined with the results of the density functional calculations to find the temperature at which each disordered structure becomes energetically favorable relative to the ground-state ordered structure. The free energy for a disordered configuration, F, is given by $F(T) = \Delta E - T\Delta S$, where $\Delta E = E_{\text{disordered}} - E_{\text{ordered}}$ is the formation energy, T is the temperature, and ΔS is the total entropy difference between the ordered and disordered configuration. The disordered structure becomes favorable relative to the ordered structure at the temperature T_0 where $F_{\text{disordered}}(T_0) \leq 0$. Contributions to entropy that are common to both the ordered and disordered structures do not affect the relative stability of the structures. We therefore assume that the entropy is dominated by configurational entropy, which we estimate using the common ideal mixing expression as a function of the concentration of disorder, x:

$$S_{\text{config}} = -2k_B \left[(1-x)\ln(1-x) + x\ln(x)\right] \qquad (1)$$

The factor of 2 comes from our independent treatment of each sub-lattice. This model excludes other possible entropic effects such as vibrational and electronic entropy, which we assume to have a much smaller relative contribution to the difference in entropy between ordered and disordered configurations. As such, the temperature obtained in this calculation is expected to form an upper bound for the true transition temperature[30].

To estimate the temperature dependence of the magnetic moment due to disorder, we used a thermodynamic average of the disordered configuration calculations. For a given temperature, T, only certain disordered configurations are energetically accessible, so the total magnetic moment M can be approximated as:

$$M(T) = \sum_i \frac{e^{-F_i(T)/(k_B T)}}{Z} m_i, \qquad (2)$$

where m_i are the calculated magnetic moments of each disordered structures, $F_i(T)$ are the free energies of these structures, and Z is the partition function of all energetically accessible structures:

$$Z = \sum_j e^{-F_j(T)/(k_B T)}. \qquad (3)$$

III. RESULTS

Figures 3 (a) and (b) show the formation energies of all defect types relative to the ordered structures. Each point on these plots represents the average of three unique SQSs. Error bars are derived from statistical standard deviation of the mean. E Solid symbols represent structures where elements on the same sub-lattice were swapped (e.g. Cu-Ni) while open symbols represent structures where elements on different sub-lattices were swapped (e.g. Cu-Mn). Swaps of Cu and Ni have a very low energy penalty likely due to similar interactions of the d states of Mn with the d states of Cu and Ni (see figure 6). The swaps with the highest energy penalty are those that substitute Cu and Ni for Al or Sn. This energy penalty is likely incurred from disrupting the specific arrangement of the *d* orbitals of Mn on the lattice or the positioning of the Al or Sn atoms which mediate these favorable interactions. The formation energies for the disordered states can be quite small, on the order of $k_B T_{RT}$ (0.025eV) per atom or less. We expect these types of low energy defects to be predominant in the alloy.

Figures 3 (c) and (d) show the total magnetic moment per atom of each disordered structure, again represented by the average of the magnetic moment per atom for three SQSs. Each point on these plots represents the total average magnetic moment per atom. The symbols are the same as in figure 3 (a) and (b). As expected, disorder across different sublattices is more detrimental to the magnetic moment than swaps of atoms on the same sublattice.

Table II shows the total magnetic moment for ordered CuNiMnAl and CuNiMnSn as well as for select disordered states. The behavior trends of the magnetic moment per atom are similar for disordered CuNiMnAl and CuNiMnSn so only those for CuNiMnAl are shown. From these values it is clear that Cu-Ni swaps have little negative effect on the exchange of electrons. Swapping of Mn-Al has little effect on the magnetic behavior of Mn but does reduce the magnetic moment of Ni. This is consistent with the conclusions of Kubler et al.[1] that, in an ordered state, both Ni and Al are likely to mediate the interaction between Mn atoms in Heusler alloys. Swaps between Mn and Al on their shared lattice are likely to keep Mn atoms well-connected (and therefore magnetic), even if Mn-Mn coupling by proximity to Ni atoms and the Ni magnetism itself is disrupted. It is also clear that as expected Cu-Mn and Mn-Ni swaps are the most detrimental to the magnetic behavior.

These results confirm that atomic disorder can have a significant effect on magnetic behavior. As predicted by Miura et al., swaps on the same sub-lattices are less detrimental to the stability of the magnetic moment than swaps across different sub-lattices. Swapping of Mn atoms with Cu or Ni atoms has the largest effect on the magnetic behavior, consistent with the hypothesis of Kubler et al. that the magnetization is caused by the precise location of Mn atoms on the lattice in relation to its neighbors[1].

TABLE II. Magnetic moments for ordered and highly disordered CuNiMnAl and CuNiMnSn

	μ_{tot}	μ_{Cu}	μ_{Ni}	μ_{Mn}	μ_{Al}
CuNiMnAl Ordered	0.91	0.0	0.33	3.33	0.0
25% Cu-Ni	0.92	0.0	0.36	3.34	0.0
25% Cu-Mn	0.73	0.0	0.31	2.61	0.0
25% Mn-Al	0.87	0.0	0.15	3.32	0.0
CuNiMnSn Ordered	0.93	0.0	0.22	3.57	0.0

Some of the disordered states do not have a high enthalpy of formation but have a substantial effect on the magnetic behavior of the alloy, i.e., Cu-Mn swapping. These lower levels of disordering can have a significant effect on the electronic behavior of the material and are likely to occur in the alloy. It cannot be assumed that annealing will remove all the disordering from the material.

These results are combined with the thermodynamic model described in Section II C to find the temperature T_0 at which each disordered structure becomes favorable relative to the ground-state structure. Figures 4 (a) and (b) are plots of the temperature T_0 vs. level of disorder for the CuNiMnAl and CuNiMnSn alloys again using the average of three SQSs. For a given swap type and level of disordering, at any temperature above that point the disordered structure is more energetically favorable than the ordered structure. From figure 4 it appears than many of the highly disordered states for CuNiMnAl become energetically accesible at a lower temperature than for CuNiMnSn. This is consistent with the XRD evidence for a higher level of disorder in CuNiMnAl than in CuNiMnSn which may show that such a threshold temperature was reached during sample preparation.

An interesting behavior to note in these plots is that some of the structures with a lower level of disorder become energetically favorable at a higher temperature than structures of the same type of swap with a higher level of disorder. This is an indication that entropic effects drive the favorability of the more disordered structures.

Using an ensemble of accessible structures the temperature dependence of magnetization was estimated for the two alloys, CuNiMnAl and CuNiMnSn. Figure 5 is a plot of magnetization vs. temperature for each of the alloys. Up to a certain temperature threshold there is increasing disorder in these structures as more disorded states become energetically accessible. Once above a certain temperature the disordered states are fully saturated. From these plots it is clear that CuNiMnSn has a larger magnetization than CuNiMnAl. Based on preliminary experimental magnetic testing, the magnetic moment of CuNiMnAl is weaker than that of CuNiMnSn, matching the behavior anticipated by this model. The scope of this discussion does not include considerations

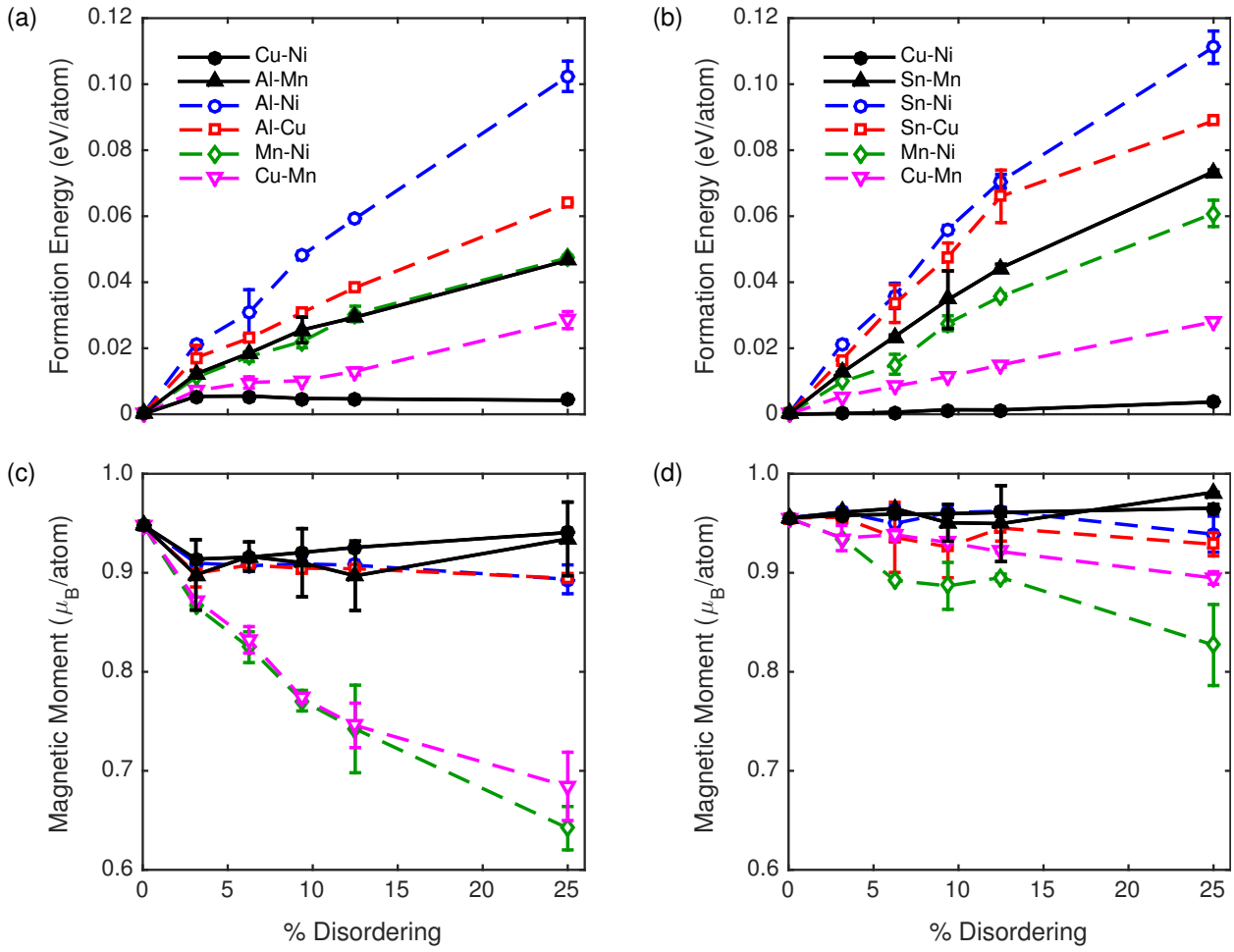

FIG. 3. Energy difference per atom between the ordered ground-state structure and the disordered structures for the average of three SQSs for (a) CuNiMnAl and (b) CuNiMnSn, and magnetic moment per atom of the ordered grounds state and the disordered structures for (c) CuNiMnAl and (d) CuNiMnSn. Swaps of elements across the same sub-lattice are represented by filled symbols and solid lines, and swaps of elements across different sub-lattices are represented by open symbols and dashed lines.

of magnetic entropy, mean field order parameter, or Curie temperature.

Figure 6 shows the total atom orbital projected spin polarized local density of states for each atom in (a) ordered CuNiMnAn, (b) ordered CuNiMnSn, (c) disordered CuNiMnAl 25% Cu-Ni and (d) CuNiMnAl with 25% Cu-Mn swapping. For ordered CuNiMnSn vs. CuNiMnAl we see a broadening of the spin down bands for Mn and Ni around -2 eV. Replacing Al with Sn shifts the Mn and Ni states and appears to open up a gap around -3 eV. This change in behavior is due the size difference between Al and Sn. Sn is slightly larger thus increasing the distance for electron exchange between Mn atoms. In these figures the Al states are not pronounced. This method for calculating the local density of states is not a perfect projection and since Al is the smallest element with the fewest electrons it is not pronounced in these plots. Figure 6 (c) shows that there is very little difference between the ordered and Cu-Ni disordered density of states, supporting the claim that the d states of the two elements interact very similarly with the d states of Mn. In 6 (d) Mn1 represents a Mn atom occupying a normal site while Mn2 represents an anti-site Mn atom. The states for this disordered structure are more pronounced and localized relative to ordered CuNiMnAl. The disorder between Cu and Mn has a significant effect on the electronic structure. This is consistent with the results Miura et al. who showed an increased effect on the DOS for swaps of atoms across different sub-lattices[18]. These types of disorder significantly impact the ability of atoms to effectively hybridize. This is due to the antiferromagnetic behavior of anti-site Mn atoms discussed further in Figure 7. The half-metallicity discussed by Hasnip[31] is not observed in these plots.

Charge density plots were also used to visualize the effect of disorder on the electronic behavior of the alloys. The converged spin-polarized charge densities were overlayed on the lattice. The difference between the spin-

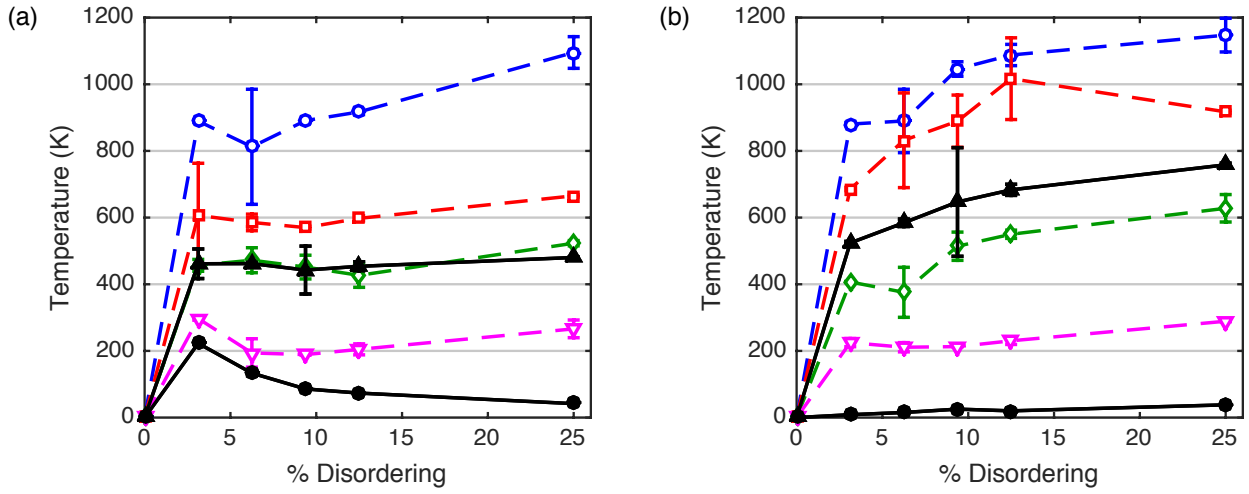

FIG. 4. Temperature vs. disordering level for the average of three SQSs for (a) CuNiMnAl and (b) CuNiMnSn. The legends are the same as those of Figures 3(a) and (b).

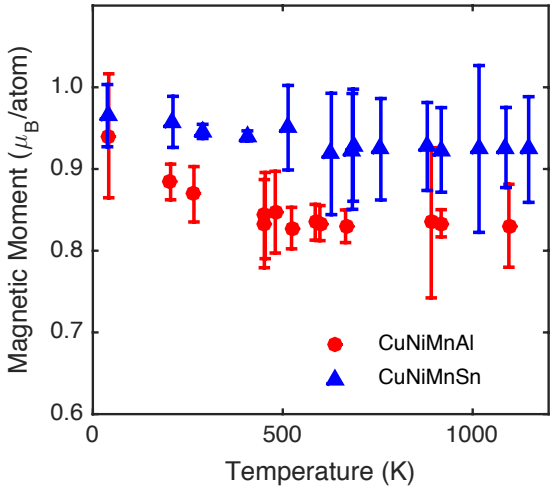

FIG. 5. Predicted magnetic moment per atom vs. temperature using the average of three SQSs for CuNiMnAl and CuNiMnSn. Each point here corresponds to a temperature where an additional disordered structure is predicted to become energetically accessible

up and spin-down density reveals localized magnetic moments, where spin-up electrons prefer to congregate while spin-down electrons localize elsewhere (and vice-versa). A perfectly ferromagnetic material might have a net positive spin charge throughout the lattice. Figure 7 shows the isosurfaces of the spin-density differences for CuNiMnAl with 25% of the Cu-Mn sites swapped. Blue corresponds to areas that are relatively more spin up, while red indicates an area that is relatively more spin down. The red area in the figure shows that anti-site Mn atoms exhibit a localized moment.

IV. SUMMARY

We have investigated the effects of atomic disordering on the electronic structure of CuNiMnAl and CuNiMnSn Heusler alloys. Six different types of atomic disordering for five different levels of disorder were explored. Swaps of atoms on the same sub-lattice were found to have a smaller effect on the magnetic behavior of the material than swaps of atoms on different sub-lattices. In both CuNiMnAl and CuNiMnSn, the clustering of the Mn atoms destroys the favorable magnetic behavior of the alloys. This confirms the influence of atomic ordering and spacing on exchange of Mn electrons and the resulting favorable magnetic properties of Mn-based Heusler alloys.

This model of atomic disordering with temperature effects corresponds well to experimental XRD results, which show a higher level of atomic order for CuNiMnSn. In addition, the predicted magnetic moment of each alloy as a function of temperature is consistent with preliminary experimental magnetic testing, showing that the magnetic moment of CuNiMnSn is stronger than that of CuNiMnAl. We have demonstrated that modeling low levels of atomic disordering and including temperature effects is a potentially powerful strategy for designing and screening Heusler alloys for spintronics applications.

The scope of this paper is restricted to heat treatment effects, not true operating temperatures. We leave calculations of Curie temperature effects for future work, as well as the inclusion of other SQSs and extension to different types of disordered structures.

ACKNOWLEDGMENTS

S.A.D., A.P.J. and L.B. acknowledge the financial support of NSF grant OISE-1261525 and the Laspa Fellow-

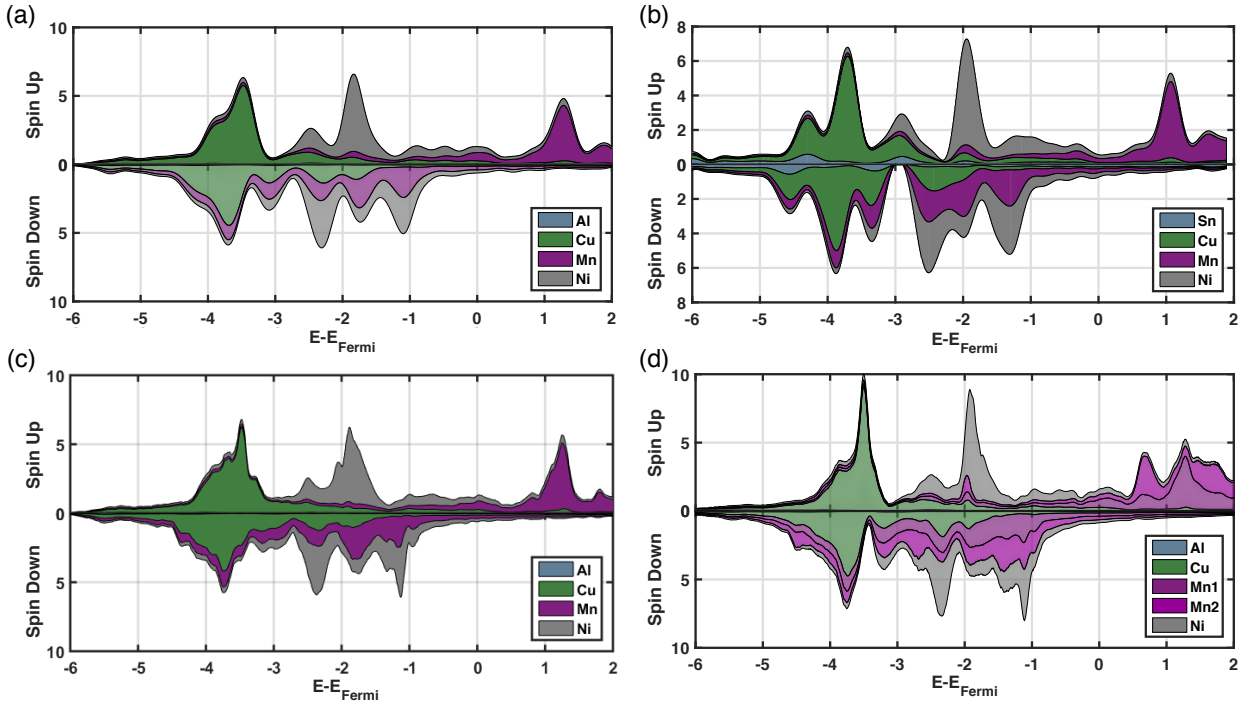

FIG. 6. Spin-resolved density of states for (a) ordered CuNiMnAl, (b) ordered CuNiMnSn (c) disordered CuNiMnAl 25% Cu-Ni and (d) disordered CuNiMnAl 25% Cu-Mn. In (d) Mn1 refers to a normal site Mn atom while Mn2 refers to an anti-site Mn atom. The x axis is the energy relative to the Fermi level.

ship at Harvey Mudd College. Thank you to Patrick Conway for contributions to the XRD analysis. We appreciate the support and assistance of M. Ferry, R. Mahjoub and P. Munroe in the School of Materials Science and Engineering at UNSW and the Mark Wainwright Analytical Centre at UNSW. A.P.J. was supported by the University of California Presidents Postdoctoral Fellowship. Part of this work was performed under the auspices of the U.S. Department of Energy by Lawrence Livermore National Laboratory under Contract DE-AC52-07NA27344. This work used the Extreme Science and Engineering Discovery Environment (XSEDE), which is supported by National Science Foundation grant number ACI-1053575.

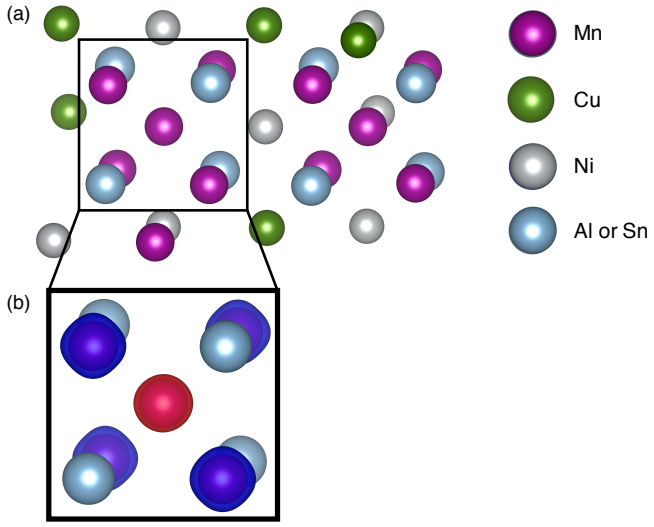

FIG. 7. (a) Site on the lattice of a Mn atom defect is outlined. (b) Iso-surface of the difference in spin-up and spin-down charge density at the location of the Mn atom usually occupied by Cu in CuNiMnAl. The isosurface value is 0.097 $e^-/\mathring{A}^3$. The center Mn has a localized spin-down charge density that contributes to a reduced overall magnetic moment in the disordered structure. Visualization created using the VESTA software package[25].

[1] J. Kübler, A. R. William, and C. B. Sommers, Phys. Rev. B **28**, 1745 (1983).
[2] A. Hirohata, H. Sukegawa, H. Yanagihara, I. Zuti, T. Seki, S. Mizukami, and R. Swaminathan, IEEE Transactions on Magnetics **51**, 1 (2015).
[3] S. Tsunegi, Y. Sakuraba, M. Oogane, K. Takanashi, and Y. Ando, Applied Physics Letters **93**, 112506 (2008).
[4] R. Shan, H. Sukegawa, W. H. Wang, M. Kodzuka, T. Furubayashi, T. Ohkubo, S. Mitani, K. Inomata, and K. Hono, Phys. Rev. Lett. **102**, 246601 (2009).
[5] Y. Sakuraba, J. Nakata, M. Oogane, Y. Ando, H. Kato, A. Sakuma, T. Miyazaki, and H. Kubota, Applied Physics Letters **88**, 022503 (2006).
[6] M. I. Katsnelson, V. Y. Irkhin, L. Chioncel, A. I. Lichtenstein, and R. A. de Groot, Rev. Mod. Phys. **80**, 315 (2008).
[7] G. A. Prinz, Science **282**, 1660 (1998).
[8] R. Topkaya, R. Yilgin, S. Kazan, N. Akdoğan, M. Obaida, H. İnam, and K. Westerholt, Journal of Superconductivity and Novel Magnetism **25**, 2605 (2011).
[9] V. V. Sokolovskiy, V. D. Buchelnikov, M. A. Zagrebin, P. Entel, S. Sahoo, and M. Ogura, Phys. Rev. B **86**, 134418 (2012).
[10] Y. Sutou, Y. Imano, N. Koeda, T. Omori, R. Kainuma, K. Ishida, and K. Oikawa, Applied Physics Letters **85**, 4358 (2004).
[11] K. Laws, C. Crosby, A. Sridhar, P. Conway, L. Koloadin, M. Zhao, S. Aron-Dine, and L. Bassman, J. Alloys Compd. **650**, 949 (2015).
[12] P. J. Webster and K. R. A. Ziebeck, "Alloys and compounds of d-elements with main group elements. part 2," (Springer, Berlin, 1988) 19c X2MnZ with X=3d element, pp. 75–184.
[13] C. Kittel, *Introduction to Solid State Physics*, eigth ed. (Wiley, 2005).
[14] S. Picozzi, A. Continenza, and A. J. Freeman, Phys. Rev. B **69**, 094423 (2004).
[15] J. A. Caballero, A. C. Reilly, Y. Hao, J. Bass, W. P. Pratt, Jr., F. Petroff, and J. R. Childress, Journal of Magnetism and Magnetic Materials **198**, 55 (1999).
[16] T. Ambrose, J. J. Krebs, and G. A. Prinz, Applied Physics Letters **76**, 3280 (2000).
[17] B. Ravel, M. P. Raphael, V. G. Harris, and Q. Huang, Phys. Rev. B **65**, 184431 (2002).
[18] Y. Miura, K. Nagao, and M. Shirai, Phys. Rev. B **69**, 144413 (2004).
[19] Y. Miura, M. Shirai, and K. Nagao, Journal of Applied Physics **99**, 08J112 (2006).
[20] Z. Gercsi and K. Hono, Journal of Physics: Condensed Matter **19**, 326216 (2007).
[21] P. J. Hasnip, J. H. Smith, and V. K. Lazarov, Journal of Applied Physics **113**, 17B106 (2013).
[22] A. van de Walle, P. Tiwary, M. de Jong, D. Olmsted, M. Asta, A. D. D. Shin, Y. Wang, L.-Q. Chen, and Z.-K. Liu, CALPHAD **42**, 13 (2013).
[23] A. van de Walle, M. Asta, and G. Ceder, CALPHAD **26**, 539 (2002).
[24] A. van de Walle, CALPHAD **33**, 266 (2009).
[25] K. Momma and F. Izumi, Journal of Applied Crystallography **41**, 653 (2008).
[26] G. Kresse and J. Furthmüller, Comput. Mater. Sci. **6**, 15 (1996).
[27] J. P. Perdew, K. Burke, and M. Ernzerhof, Phys. Rev. Lett. **77**, 3865 (1996).
[28] F. Birch, Phys. Rev. **71**, 809 (1947).
[29] G. I. Csonka, J. P. Perdew, A. Ruzsinszky, P. H. T. Philipsen, S. Lebègue, J. Paier, O. A. Vydrov, and J. G. Ángyán, Phys. Rev. B **79**, 155107 (2009).
[30] B. Burton and A. van de Walle, Chem. Geo. **225** (2006).
[31] P. J. Hasnip, K. Refson, M. I. J. Probert, J. R. Yates, S. J. Clark, and C. J. Pickard, Phil. Trans. of the R. S. A **372** (2014).